

## Two-dimensional percolation at the free water surface and its relation with the surface tension anomaly of water

Marcello Sega, George Horvai, and Pál Jedlovsky

Citation: *The Journal of Chemical Physics* **141**, 054707 (2014); doi: 10.1063/1.4891323

View online: <http://dx.doi.org/10.1063/1.4891323>

View Table of Contents: <http://scitation.aip.org/content/aip/journal/jcp/141/5?ver=pdfcov>

Published by the [AIP Publishing](#)

---

### Articles you may be interested in

[Molecular dynamics simulation of quasi-two-dimensional water clusters on ice nucleation protein](#)  
*J. Chem. Phys.* **137**, 054303 (2012); 10.1063/1.4739299

[Surface tension of water–alcohol mixtures from Monte Carlo simulations](#)  
*J. Chem. Phys.* **134**, 044709 (2011); 10.1063/1.3544926

[The surface tension of water under high magnetic fields](#)  
*J. Appl. Phys.* **103**, 124903 (2008); 10.1063/1.2940128

[Stochastic Liouville equations for hydrogen-bonding fluctuations and their signatures in two-dimensional vibrational spectroscopy of water](#)  
*J. Chem. Phys.* **123**, 114504 (2005); 10.1063/1.2008251

[Structure of the nonionic surfactant triethoxy monooctylether C 8 E 3 adsorbed at the free water surface, as seen from surface tension measurements and Monte Carlo simulations](#)  
*J. Chem. Phys.* **122**, 124704 (2005); 10.1063/1.1874872

---



**AIP** | Journal of  
Applied Physics

*Journal of Applied Physics* is pleased to  
announce **André Anders** as its new Editor-in-Chief

# Two-dimensional percolation at the free water surface and its relation with the surface tension anomaly of water

Marcello Sega,<sup>1</sup> George Horvai,<sup>2,3</sup> and Pál Jedlovsky<sup>3,4,a)</sup>

<sup>1</sup>*Department of Physics, University of Rome "Tor Vergata," via della Ricerca Scientifica 1, I-00133 Rome, Italy and Institut für Computergestützte Biologische Chemie, University of Vienna, Währinger Strasse 17, A-1090 Vienna, Austria*

<sup>2</sup>*MTA-BME Research Group of Technical Analytical Chemistry, Szt. Gellért tér 4, H-1111 Budapest, Hungary*

<sup>3</sup>*Department of Inorganic and Analytical Chemistry, Budapest University of Technology and Economics, Szt. Gellért tér 4, H-1111 Budapest, Hungary*

<sup>4</sup>*EKF Department of Chemistry, Leányka u. 6, H-3300 Eger, Hungary and Laboratory of Interfaces and Nanosize Systems, Institute of Chemistry, Eötvös Loránd University, Pázmány Péter stny. 1/a, H-1117 Budapest, Hungary*

(Received 6 June 2014; accepted 15 July 2014; published online 5 August 2014)

The percolation temperature of the lateral hydrogen bonding network of the molecules at the free water surface is determined by means of molecular dynamics computer simulation and identification of the truly interfacial molecules analysis for six different water models, including three, four, and five site ones. The results reveal that the lateral percolation temperature coincides with the point where the temperature derivative of the surface tension has a minimum. Hence, the anomalous temperature dependence of the water surface tension is explained by this percolation transition. It is also found that the hydrogen bonding structure of the water surface is largely model-independent at the percolation threshold; the molecules have, on average,  $1.90 \pm 0.07$  hydrogen bonded surface neighbors. The distribution of the molecules according to the number of their hydrogen bonded neighbors at the percolation threshold also agrees very well for all the water models considered. Hydrogen bonding at the water surface can be well described in terms of the random bond percolation model, namely, by the assumptions that (i) every surface water molecule can form up to 3 hydrogen bonds with its lateral neighbors and (ii) the formation of these hydrogen bonds occurs independently from each other. © 2014 AIP Publishing LLC. [<http://dx.doi.org/10.1063/1.4891323>]

## I. INTRODUCTION

The investigation of structural, dynamical, and energetic properties of interfaces between two fluid phases on the molecular level has been one of the most active research directions in physics, engineering, and chemistry for decades. Such investigations have been enabled by the development of several surface-sensitive experimental methods, such as second harmonic generation (SHG) and sum frequency generation spectroscopies,<sup>1</sup> or x-ray and neutron reflection measurements.<sup>2</sup> In addition, due to the rapid development of the routinely available computing capacities, computer simulation methods<sup>3</sup> have also become effective techniques that can complement the experimental investigations. In fact, using a computer simulation one can obtain an atomistic level insight into the system of interest. On the other hand, the results of simulations depend on the used model and need to be validated against experimental data.

An obvious pre-requisite of any meaningful comparison between simulation and experimental results is that the same set of molecules is probed in both approaches. Since surface sensitive experiments selectively probe molecules that are located right at the boundary of the two phases, these molecules need to be identified unambiguously also in computer simula-

tions. However, the identification of the interfacial molecules is far from being a trivial task. The surface of a fluid phase is corrugated by capillary waves, and therefore its surface cannot be defined in terms of an external (i.e., simulation box-fixed) coordinate frame. Although the majority of the early interfacial simulations simply disregarded this problem, the non-intrinsic (i.e., external frame-fixed) treatment of the fluid surface has repeatedly been shown to lead to systematic errors not only in the structure<sup>4,5</sup> or composition<sup>6–8</sup> of the surface layer but also in the thermodynamic properties of the system.<sup>9</sup>

Several methods have been proposed in the literature for identifying the truly interfacial molecules, and thus detecting the real, intrinsic (i.e., capillary wave corrugated) surface of a fluid phase. Pandit *et al.* proposed to approximate the intrinsic surface by using the two dimensional Voronoi tessellation of the surface molecules in the plane of the Gibbs dividing surface, and lift the Voronoi cells to the position of their central molecule along the interface normal axis.<sup>10</sup> However, this method still suffers from the problem of identifying the full set of the surface molecules, on which the Voronoi analysis could be performed. In their pioneering works Linse<sup>11</sup> and Benjamin<sup>12</sup> divided the simulation box into several slabs along the surface normal axis, and determined the position of the interface in each slab separately. The method was later further developed by Jorge and Cordeiro, who determined the number of slabs needed for convergence to the intrinsic

<sup>a)</sup>Electronic mail: [pali@chem.elte.hu](mailto:pali@chem.elte.hu).

surface.<sup>13</sup> Chowdhary and Ladanyi proposed another method, working solely for liquid-liquid interfaces, which is based on the proximity of molecules of the opposite phase.<sup>14</sup> The Intrinsic Sampling Method (ISM),<sup>15,16</sup> developed by Chacón and Tarazona determines the surface of minimum area going through a set of pivot atoms. The method finds the pivot atoms and the intrinsic surface simultaneously, in a self-consistent way. Further, several intrinsic methods that are even free from the assumption that the interface itself is macroscopically planar have been invented in the past decade.<sup>17–19</sup>

Recently we also proposed a method for Identifying the Truly Interfacial Molecules (ITIM),<sup>4</sup> in which the molecules being right at the interface are detected by moving spherical probes along a grid of test lines perpendicular to the macroscopic interface, starting from the bulk opposite phase. Once the probe sphere touches the first molecule in the phase of interest it is stopped, the touched molecule is marked as being interfacial, and the probe sphere starts to move along the next test line. The optimal values of the grid spacing and probe sphere size have also been determined.<sup>20</sup> It has also been shown that the above discussed intrinsic methods provide, in general, results that are consistent with each other, and that the ITIM method represents an excellent compromise between accuracy and computational efficiency.<sup>20</sup> The ITIM method has already been applied to a number of liquid-vapor<sup>4,6–8,21–26</sup> and liquid-liquid<sup>5,9,27,28</sup> interfaces.

The molecules located right at the boundary of two phases experience a rather unusual, asymmetric environment. In particular, surface water molecules practically do not interact, or interact only rather weakly, with the particles of the opposite phase in cases of the water-vapor, and water-apolar liquid-liquid interfaces, respectively. To compensate at least partly the loss of strong attractive interactions in the direction of the opposite phase, surface water molecules, similarly to waters hydrating large apolar solutes, form, on average, stronger hydrogen bonds with each other,<sup>29,30</sup> and adopt orientations that can maximize their mutual hydrogen bonding.<sup>4,5,31</sup> These effects lead naturally to an enhanced lateral connectivity of the surface water molecules. However, similarly to any other surface properties, a meaningful analysis of this lateral connectivity in computer simulations obviously requires knowing the full list of the truly interfacial molecules, and hence an intrinsic surface analysis. It has been shown by means of the ITIM method for the water-vapor<sup>4,5</sup> as well as for several water-apolar liquid-liquid interfaces<sup>5,9,27,28</sup> that the enhanced lateral hydrogen bonding results in a two-dimensional percolating network of the surface water molecules, whilst no such lateral percolating network exists in any of the molecular layers below the surface one. Using the SPC/E water model<sup>32</sup> we have previously determined the percolation threshold of the surface water molecules at the liquid-vapor interface<sup>25</sup> as well as the line of percolation (i.e., set of percolation thresholds at various pressures) at the water-benzene liquid-liquid interface,<sup>9</sup> and found that the lateral percolating network of surface waters breaks up well (i.e., about 200–400 K) below the mixing temperature of the two phases in every case.

In this paper we investigate the percolation transition of the lateral network of surface water molecules at the

water liquid-vapor interface. It is known that the three-dimensional space-filling percolating network of the bulk phase water molecules exists in the liquid phase<sup>33,34</sup> up to the critical point,<sup>35</sup> and breaks up close to,<sup>36</sup> although slightly above<sup>37,38</sup> the supercritical extension of the liquid-vapor coexistence curve. This latter finding has recently also been confirmed by experimental studies.<sup>39,40</sup> Our recent results both on the water-benzene liquid-liquid interface<sup>9</sup> and on the water liquid-vapor interface<sup>25,41</sup> showed that the breaking up of the two-dimensional lateral network of the surface molecules well precedes that of the three-dimensional space-filling network of the bulk phase water molecules. To avoid model dependence of the results we determine here the surface percolation threshold for six different water models, including three, four, and five site ones.

It is also known that the surface tension of water exhibits two points of inflection,<sup>42</sup> one around 277 K,<sup>43</sup> and another one around 530 K, i.e., about 120 K below the critical temperature<sup>44,45</sup> (see Figure 1). This behavior is one of the less studied anomalies of water. As it was written in the book of Rowlinson and Widom, “Water is unusual, first, in the particularly high values of  $\sigma$ , and second, in having a maximum in  $-(d\sigma/dT)$  at about 200 °C.”<sup>46</sup> ( $\sigma$  standing here for the surface tension). No such behavior was observed for other low-weight molecular liquids, neither for apolar (e.g., chloroform<sup>47</sup>), nor for strongly polar (e.g., acetone<sup>47</sup>), nor even for hydrogen bonding (e.g., methanol<sup>48</sup>) ones. On the other hand, it was recently shown by Bernardino and Telo da Gama that network forming polymers exhibit both inflections of the surface tension.<sup>49</sup> The low temperature inflection of water was explained using of a two-state mixture model.<sup>50</sup> We are, however, not aware of any explanation of the existence of the high temperature inflection point of the water surface tension. In a recent Letter, based on simulations with three- and four-site water models, we related this inflection with the breaking up of the spanning lateral hydrogen bonding network of the surface water molecules.<sup>41</sup> This idea is elaborated here in detail, by extending the analysis also to five-site water models. Further, we analyze the properties of the lateral

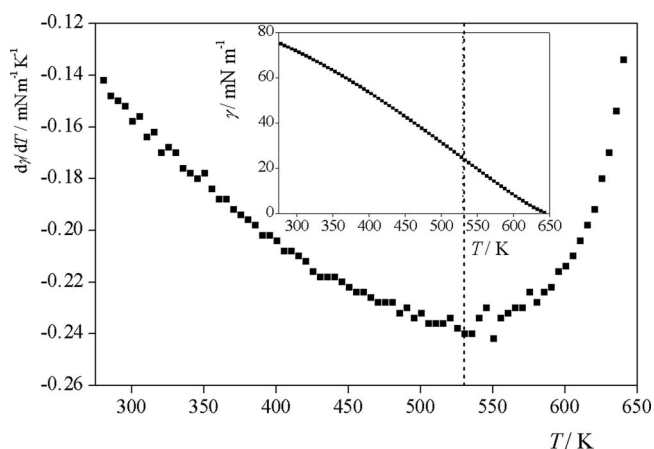


FIG. 1. Temperature derivative of the experimental surface tension of water as a function of the temperature. The minimum of this curve (i.e., the position of the surface tension inflection) is shown by a dashed vertical line. The inset shows the surface tension vs. temperature data. All data are taken from Ref. 45.

water clusters at the point of percolation, and compare the water surface percolation with the predictions of the random bond percolation model, based on the assumption of statistically independent hydrogen bond formation up to a maximum number per molecule.

The paper is organized as follows. In Sec. II details of the simulations and ITIM analysis performed are given, and the methods used to detect the percolation threshold are summarized. In Sec. III the obtained results are discussed in detail, whilst in Sec. IV the main conclusions of this study are summarized.

## II. COMPUTATIONAL DETAILS

### A. Molecular dynamics simulations and ITIM analysis

Molecular dynamics simulations of the liquid-vapor interface of water have been performed on the canonical ( $N, V, T$ ) ensemble using six different water models, namely the three site SPC<sup>51</sup> and SPC/E,<sup>32</sup> the four site TIP4P<sup>52</sup> and TIP4P/2005,<sup>53</sup> and the five site TIP5P<sup>54</sup> and TIP5P-E<sup>55</sup> ones. The critical temperatures of these models are summarized in Table I. Two sets of simulations have been performed with all these models, in which the basic simulation cell consisted of 1000 and 4000 water molecules, respectively. Each system has been simulated at 12–17 different temperatures between 300 K and the critical temperature of the model, using a 50 K temperature grid over this entire temperature interval and a 10 K grid in the vicinity of the percolation threshold. The size of the rectangular basic simulation box has been  $150.0 \times 25.0 \times 25.0$  Å in the case of the small (i.e., 1000 molecules), and  $250.0 \times 50.0 \times 50.0$  Å in the case of the large (i.e., 4000 molecules) system, the  $X$  axis being perpendicular to the macroscopic plane of the liquid-vapor interface. Standard periodic boundary conditions have been applied.

The simulations have been performed using the GRO-MACS simulation program package (version 4.5.5).<sup>61</sup> The

equations of motion have been integrated in time steps of 1 fs, keeping fixed the geometry of the water molecules by means of the SETTLE algorithm.<sup>62</sup> The temperature has been controlled by means of the Nosé-Hoover thermostat,<sup>63,64</sup> using a time constant of 2 ps. Lennard-Jones interactions have been truncated to zero beyond the cut-off distance of 10 Å; the long range part of the electrostatic interaction has been calculated using the Particle Mesh Ewald (PME) method<sup>65</sup> in its smooth variant.<sup>66</sup> The initial liquid-vapor interface has been created by enlarging along the  $X$  axis the cubic simulation boxes filled with liquid water from the initial values up to 150.0 and 250.0 Å for the small and large systems, respectively. In order to eliminate spurious dipolar interaction between periodic copies of the liquid slabs, the Yeh-Berkowitz correction<sup>67</sup> has been used. An equilibration run of 2 ns was followed by a 10 ns long production run, during which 20 000 sample configurations per system (one configuration every 0.5 ps) have been saved for subsequent analyses. To check whether the system was properly thermalized during the simulation, we calculated the temperature profile across the interface for the SPC/E model at  $T = 520$  K, which turned out to be constant at the reference temperature value throughout the liquid and vapor phase.

The water molecules constituting the surface molecular layer of the liquid phase have been identified by means of the ITIM method.<sup>4</sup> Water molecules belonging to the vapor phase have been excluded from the ITIM analysis by performing a (3D) cluster analysis: the liquid phase has been defined to be the largest water cluster in the system that is kept together by hydrogen bonds.<sup>9</sup> We would like to stress that the 3D cluster analysis performed to identify the liquid phase is a distinct procedure from the cluster analysis performed later within the surface layer to compute the spanning probabilities. For the ITIM analysis, test lines parallel to the surface normal axis,  $X$ , have been placed on a square lattice with the spacing of 0.5 Å, and a probe sphere with a radius of 1.25 Å has been employed, in accordance with the suggestions of Jorge *et al.*<sup>20</sup>

TABLE I. Critical temperature, surface percolation temperature, and temperature of the inflection of surface tension for the six water models considered. Experimental data are also included in the table. All temperature values are in K units.

Model	Critical temperature	Surface percolation temperature	Surface tension inflection temperature	
			Fitting Fermi function	Fitting third order polynomial
SPC	587 <sup>a</sup>	415 ± 5	415 ± 7	426 ± 5
SPC/E	652 <sup>b</sup>	455 ± 5	448 ± 9	462 ± 5
TIP4P	588 <sup>c</sup>	407 ± 3	413 ± 5	417 ± 3
TIP4P/2005	640 <sup>d</sup>	446 ± 5	451 ± 4	459 ± 5
TIP5P	521 <sup>c</sup>	370 ± 5	375 ± 6	382 ± 6
TIP5P-E	541 <sup>c</sup>	382 ± 3	380 ± 7	381 ± 6
Experimental	647.1 <sup>e</sup>			530 <sup>f</sup>

<sup>a</sup>Reference 56.

<sup>b</sup>Reference 57.

<sup>c</sup>Reference 58.

<sup>d</sup>Reference 59.

<sup>e</sup>Reference 60.

<sup>f</sup>Reference 45.



## B. Percolation analysis

In analyzing the surface connectivity of the water molecules we regard two waters as being hydrogen bonded to each other if their O atoms are closer to each other than 3.35 Å, and their smallest intermolecular O···H distance does not exceed 2.45 Å. These limiting distance values correspond to the first minimum position of the respective pair correlation functions at ambient conditions. Two water molecules belong to the same cluster if they are connected through an intact chain of hydrogen bonded water pairs. It should be emphasized that the present analysis is limited to the surface molecular layer of water, and non-interfacial molecules are simply disregarded. Thus, two water molecules that do not belong to the same cluster in our analysis might still well be physically connected through a chain of hydrogen bonded water pairs through the bulk region of the system. The size  $n$  of a cluster is simply the number of water molecules forming it.

The percolation threshold can be detected in several ways in computer simulations. At the percolation threshold the size distribution of the clusters,  $P(n)$ , obeys a power law,

$$P(n) \sim n^{-\alpha}, \quad (1)$$

with the exponent  $\alpha = 2.05$  in two dimensional systems.<sup>68</sup> Thus, in percolating systems the distribution  $P(n)$  exceeds the critical line up to values that are comparable with the system size (i.e., the number of water molecules being at the surface of the liquid slab in the present case). In non-percolating systems, on the contrary,  $P(n)$  drops below the critical line already at very small values of  $n$ .

Also, since the size of the largest cluster becomes comparable with the system size right at the percolation threshold, the fluctuation of the largest cluster size,

$$\sigma_{n_{\max}} = \sqrt{\langle n_{\max}^2 \rangle - \langle n_{\max} \rangle^2}, \quad (2)$$

goes through a maximum here.<sup>69</sup> In addition, the weighted average of the cluster size excluding the largest one, defined as<sup>33,68</sup>

$$n_w^* = \frac{\sum n^2 P(n)}{\sum n P(n)}, \quad (3)$$

goes through a maximum right before the percolation threshold.<sup>70</sup> In these equations the brackets  $\langle \dots \rangle$  refer to ensemble averaging, and the asterisk in Eq. (3) indicates that the largest cluster is left out from the averaging.

All these conditions allow locating the percolation threshold, but they all suffer from severe finite size effects, namely, they identify the point when the largest cluster reaches the (finite) system size rather than becoming infinite. In other words, the percolation threshold detected in any of the above ways somewhat underestimates the true percolation threshold.<sup>38</sup> A complete analysis of the finite-size scaling is, however, not needed to locate the real percolation threshold: since the largest cluster is a fractal object of a well defined dimension,<sup>68</sup> the probability of finding a cluster that spans the system is size independent at the percolation threshold, given that the dimensionality and boundary conditions of the system as well as the spanning rule are set.<sup>71</sup> Thus, the true

percolation threshold, which is free from the finite size effect error, can simply be located by identifying the temperature at which the spanning probability for two systems of different size become identical.<sup>38,72</sup> To demonstrate the robustness of this method, we use two different spanning rules in this study.  $R_1$  is the probability that the largest cluster spans the system in one dimension, whilst  $R_2$  is the probability that it spans the system in both dimensions along the macroscopic plane of the surface.

## III. RESULTS AND DISCUSSION

### A. Lateral percolation threshold and its relation with the surface tension inflection

The size distribution of the hydrogen bonding clusters at the water surface are shown in Figure 2 at the temperature where it agrees best with the critical line of Eq. (1) in the larger system simulated for all the six water models. As it has been discussed earlier, this temperature is an upper estimate of the percolation temperature, as it corresponds to the point where the size of the largest lateral cluster becomes comparable with the (finite) system size. The real, finite size effect-free percolation threshold can be identified as the point where the spanning probabilities  $R_1$  and  $R_2$  become equal for

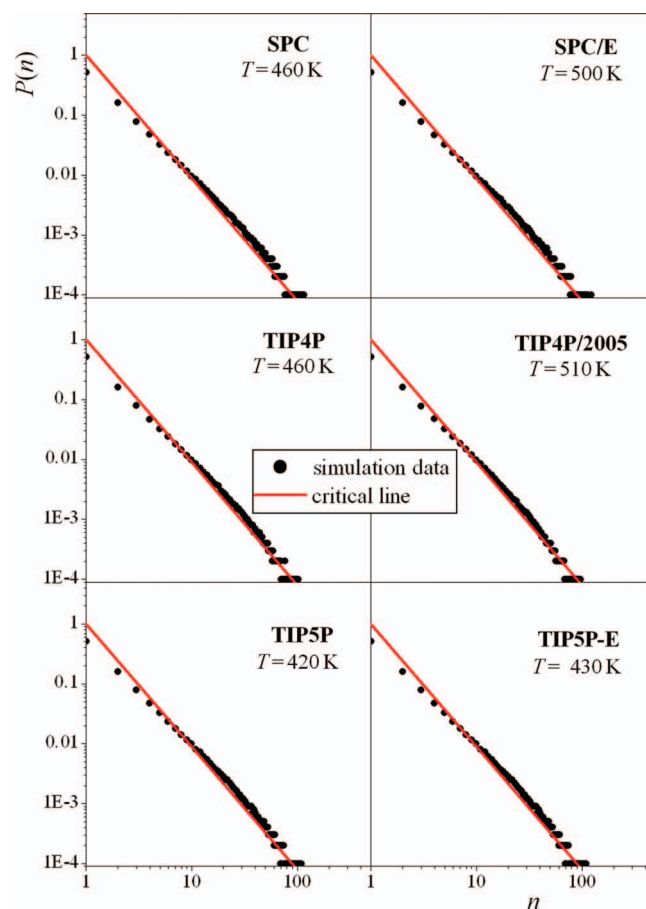


FIG. 2. Hydrogen bonded cluster size distribution in the surface layer of the large systems simulated (symbols) at the temperature where it best matches with the critical line of Eq. (1) (solid curves) for the six water models considered. The data are shown on a double logarithmic scale for better visualization.

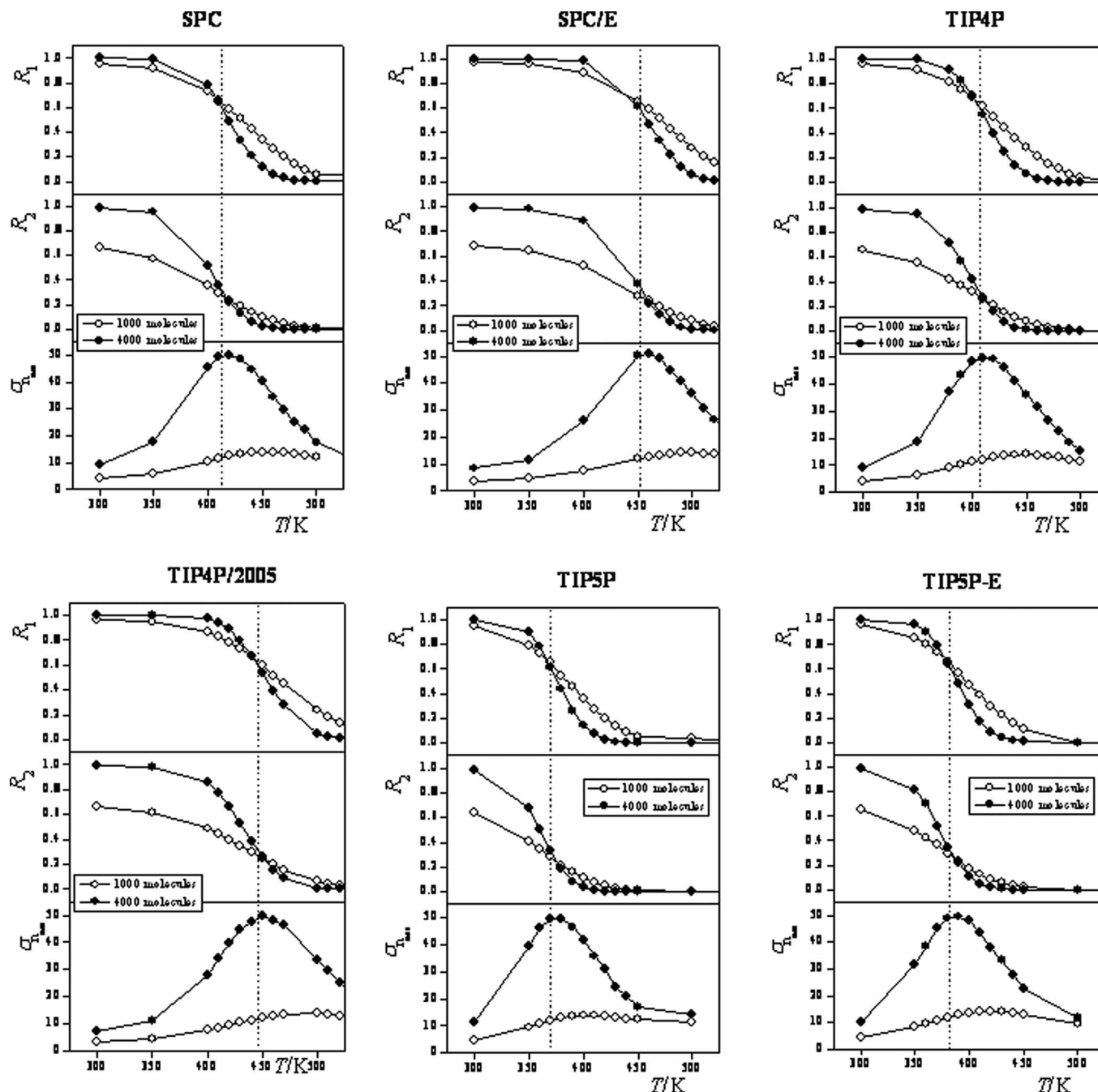


FIG. 3. One dimensional (top panels) and two dimensional (middle panels) spanning probabilities, and fluctuation of the size of the largest cluster (bottom panels) as obtained in the small (open symbols) and large (full symbols) systems at various temperatures for the six water models considered. The lines connecting the symbols are just guides to the eye. The dashed vertical line marks the percolation threshold for each water model.

two systems of different size. The temperature dependence of these spanning probabilities are shown in Figure 3 both in the small and in the large systems as obtained for all the six water models considered. The intersection of the  $R_1(T)$  and of the  $R_2(T)$  curves of the systems of different size are in every case very close (i.e., within the temperature resolution of 10 K) to each other. This intersection temperature can thus be regarded as the surface percolation threshold, namely, the point at which the infinite two dimensional hydrogen bonding network of the surface water molecules breaks up and becomes a disconnected set of finite size clusters. This real percolation temperature indeed turns out to be about 50 K lower

than the temperature at which the cluster size distribution  $P(n)$  best matches the critical line of Eq. (1) for the larger systems (see Fig. 2), and even more for the smaller systems (data not shown). The percolation temperatures of the different water models considered here are collected in Table I, together with the critical temperature values of these models. As is seen, the breaking up of the infinite network of the surface water molecules precedes the critical point by 150–200 K for all cases. More interestingly, when the surface percolation temperature is expressed in terms of reduced units, i.e., divided by the critical temperature, it falls in the range of  $0.70 \pm 0.01$  for every model.

Figure 3 also shows the temperature dependence of the fluctuation of the largest cluster size,  $\sigma_{n_{\max}}$ , (see Eq. (2)) for the systems of both sizes. As is seen, the maximum of the  $\sigma_{n_{\max}}(T)$  curve follows the percolation temperature by 5–10 K in the case of the large, and by about 50 K in the case of the small systems. This finding is again consistent with the fact that the maximum of  $\sigma_{n_{\max}}(T)$  is an upper estimate of the percolation temperature, as it is also subject to the finite size effect error, which is larger for systems of smaller size. We find rather surprising how well, in spite of this finite size effect error, the real percolation temperature can be estimated by  $\sigma_{n_{\max}}(T)$  at least in the case of the large systems.

To investigate how this lateral percolation transition is related to the surface tension inflection point, we have determined the surface tension,  $\gamma$ , for the large systems from the simulations, and fitted a third order polynomial function to the  $\gamma(T)$  data. (The surface tension curves for the small systems did not show appreciable differences for any of the six models considered, hence, we can rule out finite size effects in the surface tension calculations.) From this fit we have determined the location of the inflection point. To avoid the effect of the arbitrariness of the chosen functional form of the fitted function on the results we have repeated this procedure by using a Fermi function,

$$\gamma = B \left[ 1 - \frac{1}{1 + \exp(-C(T - T_{\text{infl}}))} \right], \quad (4)$$

instead of the polynomial, to fit the  $\gamma(T)$  data. Here  $T_{\text{infl}}$  is the temperature corresponding to the point of inflection, while  $B$  and  $C$  are further fitting parameters. The inflection temperature values determined in both ways are also collected in Table I, whereas the obtained surface tension data, together with the fitted functions, are shown in Figure 4. The values of the inflection temperature agree very well (considering the error bars and the 10 K temperature resolution used in the sets of simulations) with the temperature of the lateral percolation threshold in almost every case. It is also seen that, in general, the use of the Fermi function leads to a better match of the two temperature values.

The overall agreement between the inflection temperature and the surface percolation temperature allows us to conclude that these two temperatures coincide, and hence the inflection behavior of the water  $\gamma(T)$  data can be attributed exactly to this lateral percolation transition. Upon approaching the critical point the two coexisting phases become increasingly similar to each other, and hence the liquid phase becomes more and more gas-like. The inflection point of the surface tension is the point where the *change* of the surface tension with the temperature is of maximum. Our result thus shows that the largest step of the liquid surface towards the vapor-like structure occurs when the infinite percolating lateral network of the strongly bound surface molecules suddenly breaks up.

## B. Lateral clusters at the percolation threshold

The surface percolation temperature, similarly to other thermodynamic properties, is different for different water

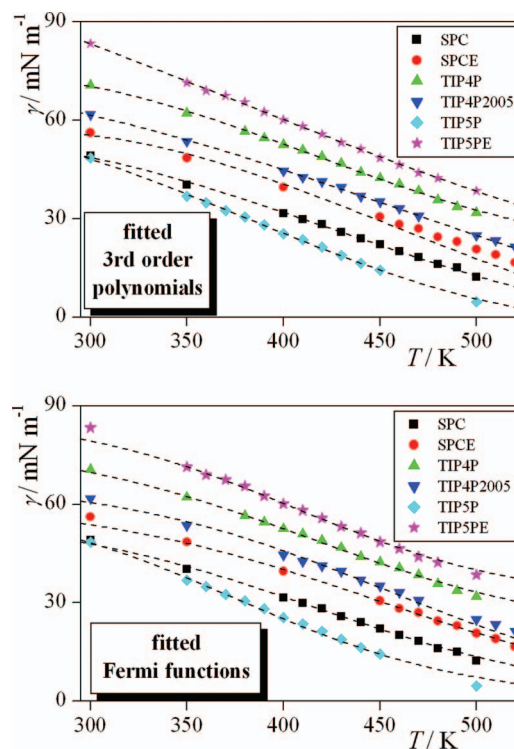


FIG. 4. Surface tension of the six water models considered as a function of the temperature, as obtained in the large systems simulated (symbols). The third order polynomials (top panel) and Fermi functions (Eq. (4), bottom panel) fitted to the  $\gamma(T)$  data are shown by dashed lines. Data corresponding to the TIP4P and TIP5P-E water models are shifted up by 20 and 30 mN/m<sup>2</sup>, respectively, for clarity.

models (see Table I). However, as it has already been noticed, this quantity is surprisingly robust if expressed in terms of reduced units, i.e., scaled by the critical temperature. It is therefore rather interesting to investigate whether the clustering structure of the surface layer right at the percolation threshold depends on the particular water model used. For this purpose, we have calculated the average number of hydrogen bonded neighbors of the water molecules within the surface layer,  $n_{\text{HB}}$ , and the fraction  $f(i)$  of the surface water molecules having exactly  $i$  hydrogen bonded neighbors ( $i$  being 0, 1, 2, 3, and 4) in the different systems. Figure 5 shows the temperature dependence of  $n_{\text{HB}}$  as obtained in systems of both sizes. Figures 6 and 7 show the  $f(i)$  distributions obtained for all the six water models in the large systems between 300 K and 500 K, and at the percolation temperature, respectively. The  $n_{\text{HB}}$  value at the percolation threshold always falls in the interval  $1.90 \pm 0.07$ . Furthermore, although the  $f(i)$  distributions of the different water models are noticeably different from each other at a given temperature, the fraction of the surface water molecules having exactly  $i$  lateral neighbors is very similar for all the six water models at the temperature of the lateral percolation threshold, being  $f(0) = 0.070 \pm 0.003$ ,  $f(1) = 0.280 \pm 0.008$ ,  $f(2) = 0.409 \pm 0.009$ ,  $f(3) = 0.217 \pm 0.005$ , and  $f(4) = 0.037 \pm 0.003$ . This finding clearly shows that, similarly to the reduced lateral percolation temperature, the clustering structure of the water surface does not depend on the particular water model used in the analysis, and appears to be an unexpectedly robust property.

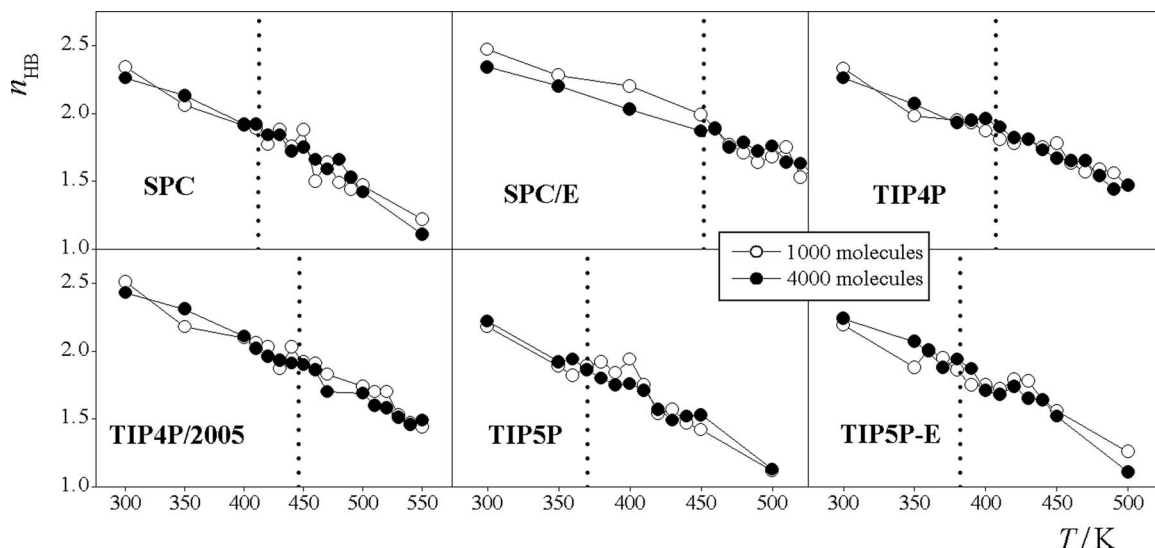


FIG. 5. Average number of hydrogen bonds a surface water molecule forms with its lateral (i.e., surface) neighbors in the small (open symbols) and large (full symbols) systems simulated at various temperatures for the six water models considered. The lines connecting the symbols are just guides to the eye. The dashed vertical line marks the percolation threshold for each water model.

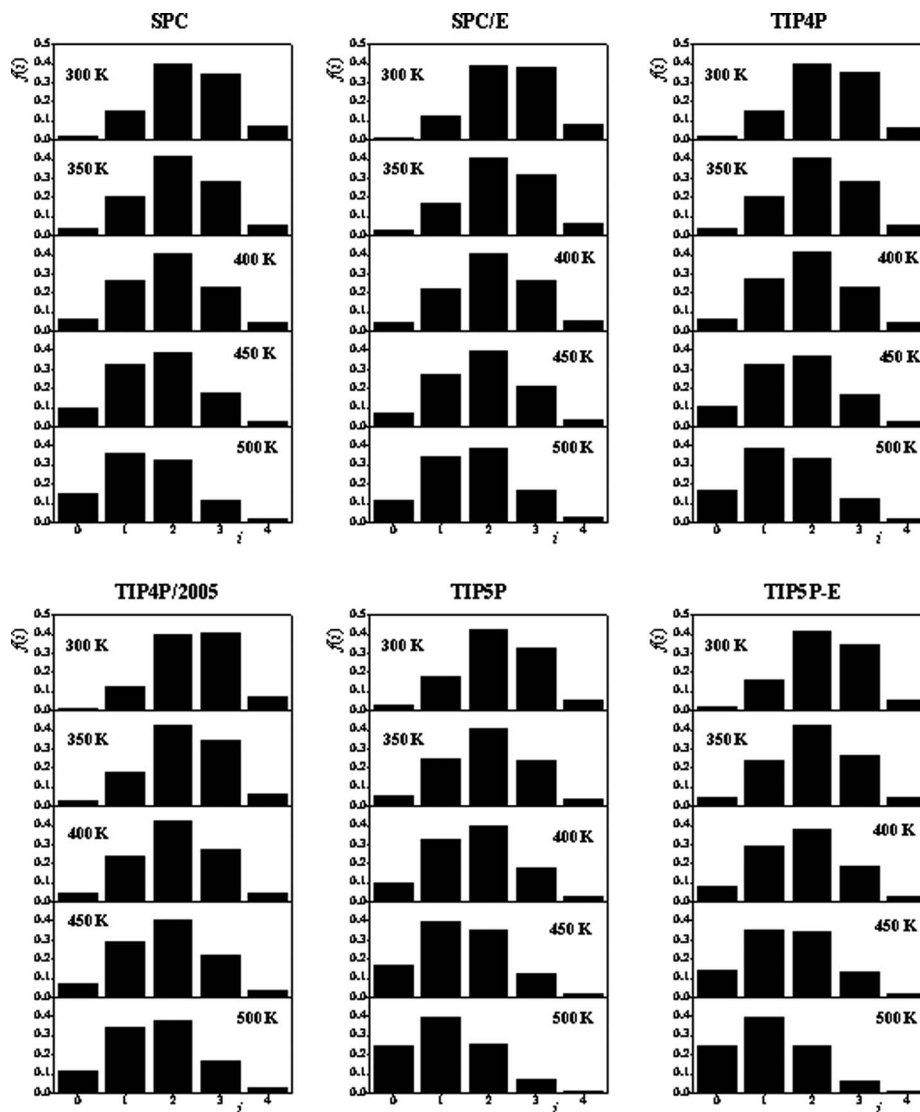


FIG. 6. Fraction of the surface water molecules having exactly  $i$  hydrogen bonded lateral (i.e., surface) neighbors in the large systems simulated at various temperatures for the six water models considered.



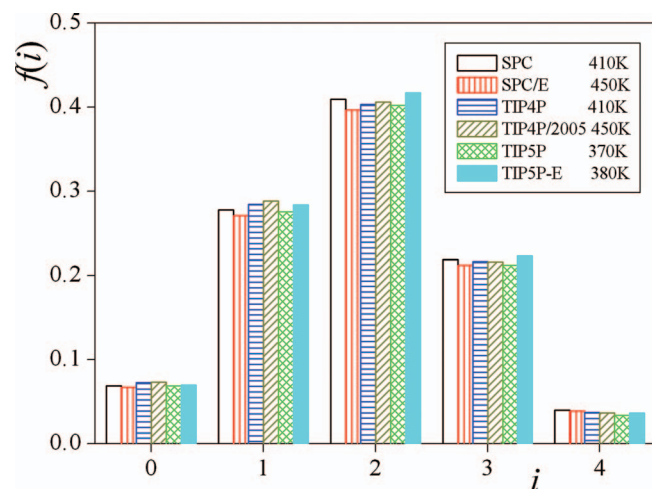


FIG. 7. Fraction of the surface water molecules having exactly  $i$  hydrogen bonded lateral (i.e., surface) neighbors in the large systems simulated at the percolation threshold for the six water models considered.

### C. Description of the lateral clusters by the random bond percolation model

The hydrogen bonding network of bulk water can be well described in terms of the random bond percolation model,<sup>73</sup> i.e., assuming that (i) every water molecule can form up to four hydrogen bonds with its neighbors and (ii) every possible hydrogen bond is formed with the same probability of  $p_{\text{HB}}$  (in other words, the probability that two neighboring molecules are hydrogen bonded to each other is independent from the presence or absence of other hydrogen bonds in the system).<sup>74,75</sup> However, as seen in Fig. 6, within the

surface layer the vast majority of the water molecules cannot form more than three hydrogen bonds with each other. Hence, to apply the random bond percolation model to the surface of water one has to assume that water molecules can form up to three (rather than four) hydrogen bonds with their lateral neighbors in the surface layer. If the two above conditions of the random bond percolation model are fulfilled, the fraction of the surface water molecules having  $i$  lateral hydrogen bonded neighbors should correspond to the Bernoulli (binomial) distribution,<sup>73–75</sup>

$$f(i) = \binom{3}{i} p_{\text{HB}}^i (1 - p_{\text{HB}})^{3-i}, \quad (5)$$

where  $p_{\text{HB}} = n_{\text{HB}}/3$  is the probability of the formation of a possible hydrogen bond.

The dependence of  $f(i)$  on  $p_{\text{HB}}$  is shown in Figure 8 for both system sizes and for all the six water models. The data sampled from the simulations follow rather well the Bernoulli distribution in every case. Considerable deviation is only seen for  $f(3)$  at large values of the hydrogen bonding probability, namely, when some of the surface water molecules (typically the ones located at the troughs, i.e., portions of locally concave curvature of the water surface<sup>4,5,31</sup>) can have four hydrogen bonded surface water neighbors. The good agreement between the simulation data and the Bernoulli distribution confirms the concept of statistically independent hydrogen bond formation also at the water surface, similarly to the case of bulk liquid water,<sup>74,75</sup> and of other non-hydrogen bonding liquids for which bonding between neighbors can only be defined through an energetic condition.<sup>76</sup>

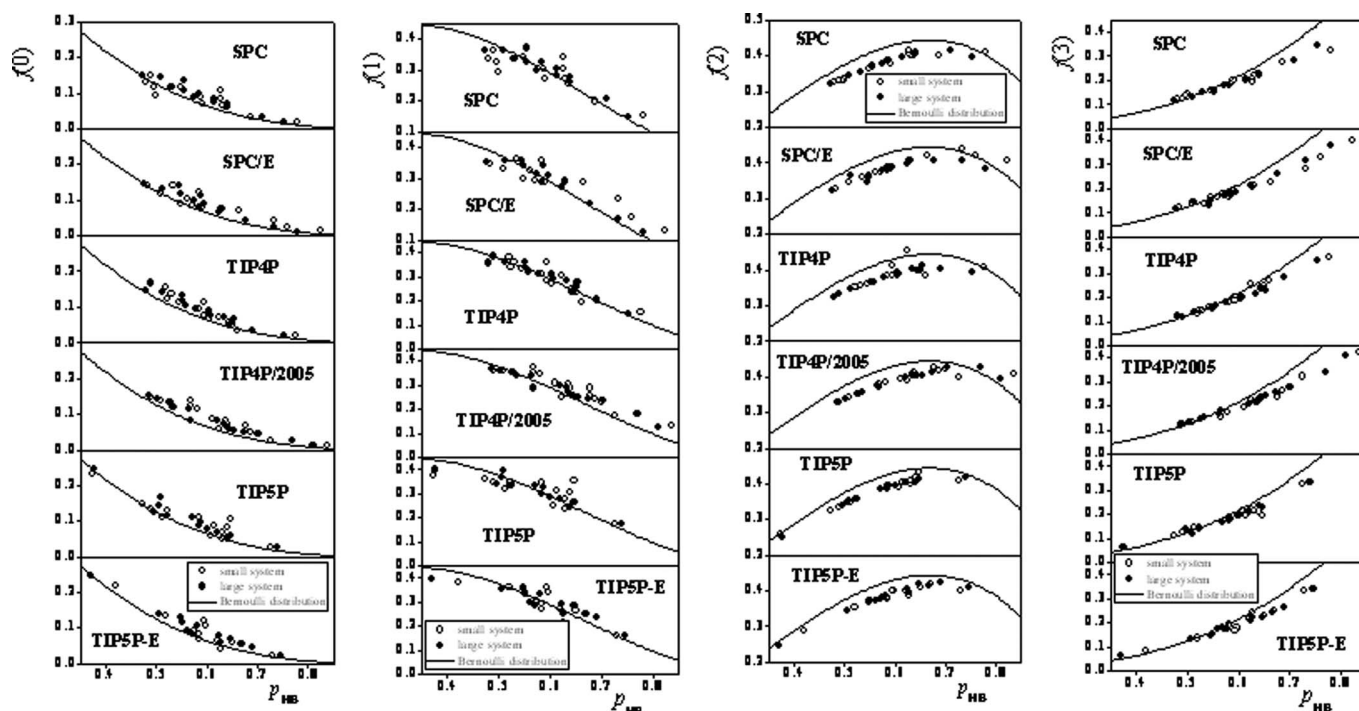


FIG. 8. Dependence of the fraction of the surface water molecules having exactly 0 (left panel), 1 (second panel), 2 (third panel), and 3 (right panel) hydrogen bonded lateral (i.e., surface) neighbors on the hydrogen bonding probability (see the text) as obtained in the small (open symbols) and large (full symbols) systems simulated for the six water models considered. The solid curves correspond to the Bernoulli distribution (see Eq. (5)).

TABLE II. Various order parameters calculated for the SPC/E model at 300 K and 450 K, and for two ideal (square and honeycomb) and one distorted (honeycomb) lattices.

Order parameter	SPC/E water		Perfect square lattice	Perfect honeycomb lattice	Distorted honeycomb lattice
	$T = 300$ K	$T = 450$ K			
$Q_4$	0.377	0.376	0.829	0.375	0.377
$Q_6$	0.315	0.315	0.586	0.741	0.338
$\Psi_6$	$0.285 - 0.060 i$	$0.278 - 0.060 i$	0	1	$0.302 - 0.061 i$

It should finally be noted that the  $p_{\text{HB}}$  value of  $0.633 \pm 0.023$ , obtained at the percolation threshold for all water models as  $n_{\text{HB}}/3$  agrees very well with the percolation threshold value of  $p_{\text{HB}} = 0.653$  of the honeycomb lattice of hexagonally arranged points.<sup>77</sup> This finding is in accordance with the fact that the (0001) cut of the  $I_h$  ice crystal also exhibits a honeycomb-like arrangement of the surface molecules, and suggests that, in analogy with their distorted random tetrahedral network in the bulk liquid phase, water molecules are arranged in a distorted random honeycomb network at the water surface.

In order to add more means of quantitative comparison, we calculated several order parameters within the surface layer (projecting the position of the surface oxygen atoms on the macroscopic surface plane,  $YZ$ ). In Table II we report the averaged Steinhardt 4-fold and 6-fold order parameters  $Q_4$  and  $Q_6$ ,<sup>78</sup> computed using the code of Wang and co-workers,<sup>79</sup> and defined as

$$Q_l = \sqrt{\frac{4\pi}{2l+1} \sum_{m=-l}^l |\bar{Q}_{lm}|^2}, \quad (6)$$

where

$$\bar{Q}_{lm} = \frac{1}{N_k} \sum_{k=1}^{N_n} Y_{lm}(\theta_k, \phi_k), \quad (7)$$

and where  $N_n$  is the number of neighbors, and  $\theta_k$  and  $\phi_k$  are the polar and azimuthal angles of bond  $k$  with respect to an arbitrary reference system. Finally,  $Y_{lm}$  are the standard spherical harmonics, and the order parameters have been averaged over all atoms in the surface layers, and over all sampled configurations. In addition to the Steinhardt order parameters, we have also calculated also the Mermin order parameter,<sup>80</sup>

$$\Psi_6 = \frac{1}{N_n} \sum_{k=1}^{N_n} \exp(i6\theta_k), \quad (8)$$

where  $\theta_k$  is the angle between the  $k$ th and the first neighbor, and again the parameter has been averaged over all surface O atoms and configurations. In Table II we report the values of all these three order parameters as calculated from our simulations with the SPC/E model at 300 and 450 K, and compare them with the values corresponding to the exact square lattice, exact honeycomb lattice, and a distorted honeycomb lattice, in which the lattice points have been randomly displaced by  $\pm 35\%$  from their position in the perfect lattice. The obtained values clearly confirm our conclusion that the molecules at the surface of liquid water form a distorted honeycomb lat-

tice, in a clear analogy with the distorted tetrahedral network of the water molecules in the bulk liquid phase.

#### IV. SUMMARY AND CONCLUSIONS

We have analyzed the breaking up of the infinite lateral percolating hydrogen-bonding network of the molecules at the surface of liquid water on the basis of computer simulations with six different water models. We found that this lateral percolating network breaks up 150–200 K below the critical point for each model. The structure of the hydrogen bonding clusters at the water surface turned out to be model independent at the percolation threshold: here the water molecules have, on average,  $1.90 \pm 0.07$  hydrogen bonded neighbors within the surface layer, and about  $7.0 \pm 0.3$ ,  $28.0 \pm 0.8$ ,  $40.9 \pm 0.9$ ,  $21.7 \pm 0.5$ , and  $3.7 \pm 0.3\%$  of them have 0, 1, 2, 3, and 4 hydrogen bonded lateral neighbors, respectively. We also found that the random bond percolation model<sup>73</sup> describes well the hydrogen bonding at the water surface.

Clearly the most important finding of this study is, however, that the lateral percolation temperature of the surface coincides with the surface tension inflection temperature of water, and hence the anomalous behavior of the water surface tension (i.e., the presence of the inflection) is explained by the transition from a percolating to a non-percolating hydrogen-bonded network of the surface molecules. Thus, the decrease of the surface tension with temperature parallels the decreasing cohesion of the water molecules within the surface layer. The decrease of this in-layer cohesion is clearly the largest at the point where the infinite lateral network of the hydrogen bonding molecules breaks up into small finite hydrogen bonding clusters. The largest decrease of the cohesion within the surface layer corresponds to the largest decrease of the surface tension with temperature, i.e., the inflection of the surface tension vs. temperature data. The excellent agreement of the inflection and lateral percolation temperatures for all the six water models considered here clearly confirms this explanation. On a side note, we thought initially that this robustness could be the hint of an underlying universal behavior of the surface tension, but we did not manage to find a suitable master curve. There is indeed a universal behavior, which is, however, related to the geometric nature of the percolation transition: this is clearly seen in the almost perfect agreement between the distributions of hydrogen-bonded partners at the percolation temperature. The universality, however, is lost as soon as the temperature deviates from the percolation threshold, and the differences between the models start showing up in the temperature dependence of the surface tension.

It should finally be noted that this explanation of the surface tension anomaly of water required inherently an intrinsic treatment of the water surface in the computer simulation, as the investigation of lateral percolation within the surface layer can only be done if the surface layer itself is already accurately identified. This result clearly stresses the importance of intrinsic analysis of fluid surfaces in computer simulations, and also well demonstrates that, in spite of several claims of the contrary, the concept of the intrinsic surface is clearly more than simply a theoretical construction, as it is needed to explain certain experimental observations.

## ACKNOWLEDGMENTS

This work has been supported by the Hungarian OTKA Foundation under Project No. 104234 and by the MTA-CNR bilateral grant. P.J. is a Szentágotthai János fellow of Hungary, supported by the European Union, co-financed by the European Social Fund in the framework of TÁMOP 4.2.4.A/2-11/1-2012-0001 “National Excellence Program” under Grant No. A2-SZJÖ-TOK-13-0030. M.S. acknowledges support from the European Community’s Seventh Framework Programme (FP7-PEOPLE-IEF) funded under Grant Agreement No. 331932 SIDIS.

- <sup>1</sup>G. L. Richmond, *Chem. Rev.* **102**, 2693 (2002).
- <sup>2</sup>J. Daillant and A. Gibaud, *X-Ray and Neutron Reflectivity: Principles and Applications* (Springer, Berlin, 1999).
- <sup>3</sup>M. P. Allen and D. J. Tildesley, *Computer Simulations of Liquids* (Clarendon, Oxford, 1987).
- <sup>4</sup>L. B. Pártay, Gy. Hantal, P. Jedlovsky, Á. Vincze, and G. Horvai, *J. Comput. Chem.* **29**, 945 (2008).
- <sup>5</sup>Gy. Hantal, M. Darvas, L. B. Pártay, G. Horvai, and P. Jedlovsky, *J. Phys.: Condens. Matter* **22**, 284112 (2010).
- <sup>6</sup>L. B. Pártay, P. Jedlovsky, Á. Vincze, and G. Horvai, *J. Phys. Chem. B* **112**, 5428 (2008).
- <sup>7</sup>L. B. Pártay, P. Jedlovsky, and G. Horvai, *J. Phys. Chem. C* **113**, 18173 (2009).
- <sup>8</sup>K. Pojžák, M. Darvas, G. Horvai, and P. Jedlovsky, *J. Phys. Chem. C* **114**, 12207 (2010).
- <sup>9</sup>L. B. Pártay, G. Horvai, and P. Jedlovsky, *J. Phys. Chem. C* **114**, 21681 (2010).
- <sup>10</sup>A. S. Pandit, D. Bostick, and M. L. Berkowitz, *J. Chem. Phys.* **119**, 2199 (2003).
- <sup>11</sup>P. Linse, *J. Chem. Phys.* **86**, 4177 (1987).
- <sup>12</sup>I. Benjamin, *J. Chem. Phys.* **97**, 1432 (1992).
- <sup>13</sup>M. Jorge and M. N. D. S. Cordeiro, *J. Phys. Chem. C* **111**, 17612 (2007).
- <sup>14</sup>J. Chowdhary and B. M. Ladanyi, *J. Phys. Chem. B* **110**, 15442 (2006).
- <sup>15</sup>E. Chacón and P. Tarazona, *Phys. Rev. Lett.* **91**, 166103 (2003).
- <sup>16</sup>E. Chacón and P. Tarazona, *J. Phys.: Condens. Matter* **17**, S3493 (2005).
- <sup>17</sup>M. Mezei, *J. Mol. Graphics Modell.* **21**, 463 (2003).
- <sup>18</sup>A. P. Wilard and D. Chandler, *J. Phys. Chem. B* **114**, 1954 (2010).
- <sup>19</sup>M. Sega, S. S. Kantorovich, P. Jedlovsky, and M. Jorge, *J. Chem. Phys.* **138**, 044110 (2013).
- <sup>20</sup>M. Jorge, P. Jedlovsky, and M. N. D. S. Cordeiro, *J. Phys. Chem. C* **114**, 11169 (2010).
- <sup>21</sup>M. Darvas, K. Pojžák, G. Horvai, and P. Jedlovsky, *J. Chem. Phys.* **132**, 134701 (2010).
- <sup>22</sup>G. Hantal, M. N. D. S. Cordeiro, and M. Jorge, *Phys. Chem. Chem. Phys.* **13**, 21230 (2011).
- <sup>23</sup>M. Lísál, Z. Posel, and P. Izák, *Phys. Chem. Chem. Phys.* **14**, 5164 (2012).
- <sup>24</sup>G. Hantal, I. Voroshylova, M. N. D. S. Cordeiro, and M. Jorge, *Phys. Chem. Chem. Phys.* **14**, 5200 (2012).
- <sup>25</sup>M. Darvas, G. Horvai, and P. Jedlovsky, *J. Mol. Liq.* **176**, 33 (2012).
- <sup>26</sup>M. Lísál and P. Izák, *J. Chem. Phys.* **139**, 014704 (2013).
- <sup>27</sup>L. B. Pártay, G. Horvai, and P. Jedlovsky, *Phys. Chem. Chem. Phys.* **10**, 4754 (2008).
- <sup>28</sup>Gy. Hantal, P. Terleczy, G. Horvai, L. Nyulászi, and P. Jedlovsky, *J. Phys. Chem. C* **113**, 19263 (2009).
- <sup>29</sup>M. Mezei and D. L. Beveridge, *J. Chem. Phys.* **74**, 622 (1981).
- <sup>30</sup>P. Jedlovsky, *J. Phys.: Condens. Matter* **16**, S5389 (2004).
- <sup>31</sup>P. Jedlovsky, M. Předota, and I. Nezbeda, *Mol. Phys.* **104**, 2465 (2006).
- <sup>32</sup>H. J. C. Berendsen, J. R. Grigera, and T. P. Straatsma, *J. Phys. Chem.* **91**, 6269 (1987).
- <sup>33</sup>A. Geiger, F. H. Stillinger, and A. Rahman, *J. Chem. Phys.* **70**, 4185 (1979).
- <sup>34</sup>H. E. Stanley and J. Teixeira, *J. Chem. Phys.* **73**, 3404 (1980).
- <sup>35</sup>P. Jedlovsky, R. Vallauri, and J. Richardi, *J. Phys.: Condens. Matter* **12**, A115 (2000).
- <sup>36</sup>L. Pártay and P. Jedlovsky, *J. Chem. Phys.* **123**, 024502 (2005).
- <sup>37</sup>L. B. Pártay, P. Jedlovsky, I. Brovchenko, and A. Oleinikova, *Phys. Chem. Chem. Phys.* **9**, 1341 (2007).
- <sup>38</sup>L. B. Pártay, P. Jedlovsky, I. Brovchenko, and A. Oleinikova, *J. Phys. Chem. B* **111**, 7603 (2007).
- <sup>39</sup>M. Bernabei, A. Botti, F. Bruni, M. A. Ricci, and A. K. Soper, *Phys. Rev. E* **78**, 021505 (2008).
- <sup>40</sup>M. Bernabei and M. A. Ricci, *J. Phys.: Condens. Matter* **20**, 494208 (2008).
- <sup>41</sup>M. Sega, G. Horvai, and P. Jedlovsky, *Langmuir* **30**, 2969 (2014).
- <sup>42</sup>J. Pellicer, V. García-Morales, L. Guanter, M. J. Hernández, and M. Dolz, *Am. J. Phys.* **70**, 705 (2002).
- <sup>43</sup>P. T. Hacker, “Experimental values of the surface tension of supercooled water,” Technical Note 2510, National Advisory Committee for Aeronautics, 1951.
- <sup>44</sup>N. B. Vargaftik, B. N. Volkov, and L. D. Voljak, *J. Phys. Chem. Ref. Data* **12**, 817 (1983).
- <sup>45</sup>IAPWS, “Release on surface tension of ordinary water substance,” 1994, see <http://www.iapws.org/relguide/surf.pdf>.
- <sup>46</sup>J. S. Rowlinson and B. Widom, *Molecular Theory of Capillarity* (Dover Publications, Mineola, 2002), p. 11.
- <sup>47</sup>See <http://www.ddbst.com> for Dortmund Data Bank.
- <sup>48</sup>M. Součková, J. Klomfar, and J. Pátek, *J. Chem. Eng. Data* **53**, 2233 (2008).
- <sup>49</sup>N. R. Bernardino and M. M. Telo da Gama, *Phys. Rev. Lett.* **109**, 116103 (2012).
- <sup>50</sup>J. Hrubý and V. Holten, “A two-structure model of thermodynamic properties and surface tension of supercooled water,” in *14th International Conference on Properties Water Steam*, Kyoto, 2004.
- <sup>51</sup>H. J. C. Berendsen, J. P. M. Postma, W. F. van Gunsteren, and J. Hermans, in *Intermolecular Forces*, edited by B. Pullman (Reidel, Dordrecht, 1981), p. 331.
- <sup>52</sup>W. L. Jorgensen, J. Chandrasekhar, J. D. Madura, R. W. Impey, and M. L. Klein, *J. Chem. Phys.* **79**, 926 (1983).
- <sup>53</sup>J. L. F. Abascal and C. Vega, *J. Chem. Phys.* **123**, 234505 (2005).
- <sup>54</sup>M. Mahoney and W. L. Jorgensen, *J. Chem. Phys.* **112**, 8910 (2000).
- <sup>55</sup>S. W. Rick, *J. Chem. Phys.* **120**, 6085 (2004).
- <sup>56</sup>J. J. de Pablo, J. M. Prausnitz, H. J. Strauch, and P. T. Cummings, *J. Chem. Phys.* **93**, 7355 (1990).
- <sup>57</sup>Y. Guissani and B. Guillot, *J. Chem. Phys.* **98**, 8221 (1993).
- <sup>58</sup>M. Lísál, I. Nezbeda, and W. R. Smith, *J. Phys. Chem. B* **108**, 7412 (2004).
- <sup>59</sup>C. Vega, J. L. F. Abascal, and I. Nezbeda, *J. Chem. Phys.* **125**, 034503 (2006).
- <sup>60</sup>L. Haar, J. S. Gallagher, and G. S. Kell, *NBS/NRC Steam Tables* (Hemisphere, New York, 1984).
- <sup>61</sup>B. Hess, C. Kutzner, D. van der Spoel, and E. Lindahl, *J. Chem. Theory Comput.* **4**, 435 (2008).
- <sup>62</sup>S. Miyamoto and P. A. Kollman, *J. Comput. Chem.* **13**, 952 (1992).
- <sup>63</sup>S. Nosé, *Mol. Phys.* **52**, 255 (1984).
- <sup>64</sup>W. G. Hoover, *Phys. Rev. A* **31**, 1695 (1985).
- <sup>65</sup>T. Darden, D. York, and L. Pedersen, *J. Chem. Phys.* **98**, 10089 (1993).
- <sup>66</sup>U. Essman, L. Perera, M. L. Berkowitz, T. Darden, H. Lee, and L. G. Pedersen, *J. Chem. Phys.* **103**, 8577 (1995).
- <sup>67</sup>I. C. Yeh and M. L. Berkowitz, *J. Chem. Phys.* **111**, 3155 (1999).
- <sup>68</sup>D. Stauffer, *Introduction to Percolation Theory* (Taylor and Francis, London, 1985).
- <sup>69</sup>I. Brovchenko, A. Krukau, A. Oleinikova, and A. K. Mazur, *J. Phys. Chem. B* **111**, 3258 (2007).
- <sup>70</sup>A. Oleinikova, I. Brovchenko, A. Geiger, and B. Guillot, *J. Chem. Phys.* **117**, 3296 (2002).
- <sup>71</sup>J. P. Hovi and A. Aharony, *Phys. Rev. E* **53**, 235 (1996).

- <sup>72</sup>J. Skvor, I. Nezbeda, I. Brovchenko, and A. Oleinikova, [Phys. Rev. Lett.](#) **99**, 127801 (2007).
- <sup>73</sup>D. Stauffer, [Phys. Rep.](#) **54**, 1 (1979).
- <sup>74</sup>M. Mezei, [Mol. Phys.](#) **52**, 1003 (1984).
- <sup>75</sup>R. L. Blumberg, H. E. Stanley, A. Geiger, and P. Mausbach, [J. Chem. Phys.](#) **80**, 5230 (1984).
- <sup>76</sup>G. Pálincás and P. Jedlovsky, [Chem. Phys.](#) **185**, 173 (1994).
- <sup>77</sup>M. F. Sykes and J. W. Essam, [J. Math. Phys.](#) **5**, 1117 (1964).
- <sup>78</sup>P. J. Steinhardt, D. R. Nelson, and M. Ronchetti, [Phys. Rev. B](#) **28**, 784 (1983).
- <sup>79</sup>Y. Wang, S. Teitel, and C. Dellago, [J. Chem. Phys.](#) **122**, 214722 (2005).
- <sup>80</sup>N. D. Mermin, [Phys. Rev.](#) **176**, 250 (1968).